

An entropic approach for evaluation of surface roughness uniformity

Pires M. A¹; Figueiredo S.S. ¹; Prioli R²; Zamora R.R.M.¹

¹ *University Federal of Amapá, Macapá, AP, Brazil*

² *Pontifícia Universidade Católica, Rio de Janeiro, RJ, Brazil*

robert@unifap.br

Surface roughness plays a crucial role in tribology. In order to make an accurate evaluation of one of the most common measure, roughness RMS, R_q , it is essential to have a high surface roughness uniformity. In this paper, we introduce the Shannon entropy as a measure of surface roughness uniformity. For numerically-generated randomly rough surface, we compare the performance of evaluating this measure from the height distribution, $H_{hei.dist}$ and from the height matrix, $H_{hei.matr}$. The results show that $H_{hei.matr}$ is more sensitive to surface roughness uniformity than $H_{hei.dist}$. Moreover, $H_{hei.dist}$ and R_q are negatively correlated, while $H_{hei.matr}$ and R_q are uncorrelated. Additionally, $H_{hei.dist}$ depends on an additional parameter, the size of bin, in the discretization of height distribution, whereas $H_{hei.matr}$ is parameter free. These results imply that $H_{hei.matr}$ is better suited for the investigation of surface roughness uniformity than $H_{hei.dist}$ complementing the information of R_q .

1. Introduction

Studying of surface roughness is very important in understanding several physics phenomena such as friction [1], adhesion [2], and so on. Moreover, surface roughness has a considerable practical importance for nanocomposites and nanostructured materials [3], development of small mechanical devices [4], self-cleaning surfaces [5], among others.

From the topography one can extract the RMS (Root Mean Square) roughness parameter, R_q , which can be easily calculated and it is widely used to quantify surface roughness even though it suffers from some disadvantages [6, 7]. The measure R_q can be biased if the surface has a considerably number of high peaks or deep valleys, relatively to the mean height. That is, the R_q can be affected if the roughness is not uniformly distributed on the entire surface. In this perspective, it is important to evaluate the surface roughness uniformity. To this purpose, we propose applying the Shannon entropy [8] as a surface roughness uniformity measure.

Recently, Nosonovsky [9] introduced the Shannon entropy as a measure of randomness for rough profiles, where he assumes that each data point (pixel) corresponds to a bin. In

our approach we consider the Shannon entropy as a measure of uniformity of the entire surface and we compare the computation of this entropy employing the height distribution and the height matrix. Henceforth, $H_{hei.matr}$ denotes the estimation of the Shannon entropy from the topographic height matrix and $H_{hei.dist}$ denotes the estimation of the Shannon entropy from the topographic height distribution.

The relationship between data uniformity and entropy has been successfully applied in several fields of science such as economy [10], electromyography and kinesiology [11], operational research [12], clinical radiology [13], manufacturing [14]. For instance, Kam et al. (2012) identifies several uniformity metrics from several areas and compares their performance in detecting nonuniform particle distributions. They show that Shannon entropy is the recommended measure for assessing spatial uniformity of particle distributions on surface [15]. As this distribution is discrete, the use of Shannon entropy is straightforward. However, applying this measure for a continuum distribution requires more effort. This is the case

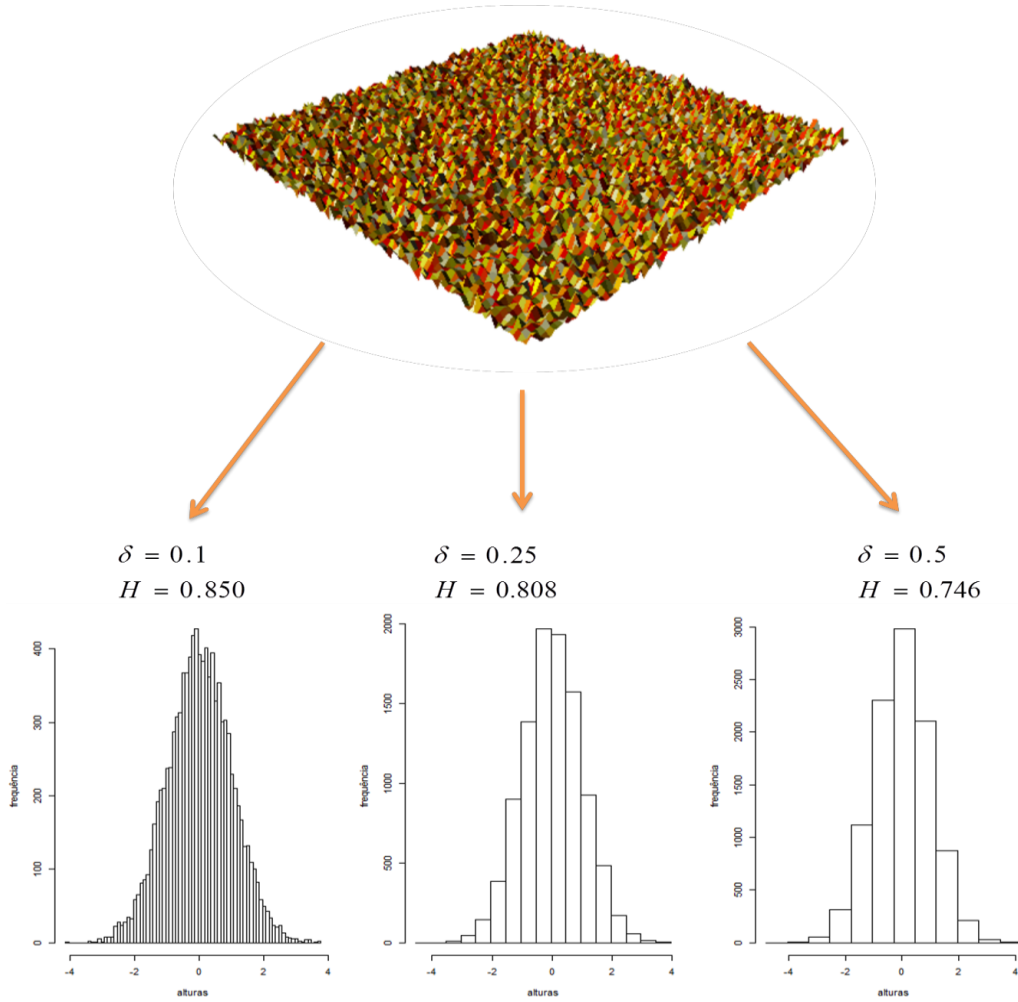


Figure 1 Application of $H_{hei.dist}$ for surface characterization suffer from dependence of such measure on δ . In this case, it is shown (from top to bottom) a random rough surface and its corresponding height distribution with three choices of δ that lead to three $H_{hei.dist}$.

of height distribution function.

In order to estimate $H_{hei.dist}$ one needs to discretize the height distribution into bins of size δ . Nonetheless, one can take distinct $H_{hei.dist}$ as a result of different choices of δ for a given surface. In order to overcome this weakness of $H_{hei.dist}$ we replace the height distribution by the height matrix in evaluation of topographic entropy, $H_{hei.matr}$.

The remainder of the paper is organized as follows. We start Section 2 by describing how computing $H_{hei.dist}$ (Subsection 2.1) and outlining the procedure for evaluating $H_{hei.matr}$ (Subsection 2.2). After that, we delineate the numerical simulation used to evaluate which is the procedure, $H_{hei.dist}$ or $H_{hei.matr}$, better suited for quantifying surface roughness uniformity (Subsection 2.3). In Section 3, we present results and discussions for the numerical simulation described above. In Section 4, we summarize the paper and we consider possible further works.

2. Topographic Uniformity

From the topographic perspective, a surface is completely characterized by a single matrix, the height matrix, whose entries h_{ij} are the height of corresponding data points (or pixels) located at (x_i, y_j) or just (i, j) . The height matrix can be extracted, for instance, by imaging techniques [6].

2.1 Topographic Entropy from height distribution

Once the height matrix is extracted, one can apply the histogram method to obtain the discretized height distribution with B bins of size δ each one.

Thereafter, we compute the probability p_k of appearance of a height in the bin k

$$p_k = \frac{n_k}{\sum_{k=1}^B n_k} \quad (1)$$

where n_k stands for the number of heights in the bin k .

The topographic entropy is taken as the Shannon entropy,

$$H^{(1)} = -\sum_{k=1}^B p_k \log p_k \quad (2)$$

Its normalized and centralized value is

$$H_{hei.dist} = -\sum_{k=1}^B \frac{p_k \log p_k}{\log B} \quad (3)$$

Since $0 \leq H^{(1)} \leq \log B$. The value $H^{(1)}=\log B$ occurs for uniform height distribution where $p_k=1/B$, on the other side $H^{(1)}=0$ occurs when $B=1$ and $p=1$.

The discretization process described above depends on the size δ . Different choices of δ can lead to different quantities of B and n_k . As a result of this, one can take different $H_{hei.dist}$ for the same surface as illustrated in Fig.1. One would expect that this limitation of $H_{hei.dist}$ could be solved by choosing the minimum δ allowed by binning process, $\tilde{\delta}_{min}$. Nonetheless, even so $H_{hei.dist}$ could be δ -case dependent because different surfaces can have different $\tilde{\delta}_{min}$.

2.2 Topographic Entropy from height matrix

As the topographic entropy is related to the degree of surface roughness uniformity we assume that to evaluate how uniform a surface is we need to know whether the height h_{ij} contribute or not to the uniformity. To help in this task we estimate the first and third quantiles Q_1 and Q_3 . Next, we compute the quantities $\tilde{Q}_1 = Q_1 - 1.5|Q_3 - Q_1|$ and $\tilde{Q}_3 = Q_3 + 1.5|Q_3 - Q_1|$ that represents whiskers in the statistical boxplot.

We assume that the contribution to the uniformity comes from the set of pixels whose height h_{ij} belongs to the region $[\tilde{Q}_1, \tilde{Q}_3]$, on the other hand the pixels whose $h_{ij} \notin [\tilde{Q}_1, \tilde{Q}_3]$ have no contribution. We denote by η the pixels that has no contribution to the uniformity. The smaller the value of η , the more uniform is the surface. When $\eta=0$, one has a uniform surface.

$$\omega_{ij} = \begin{cases} 1, & h_{ij} \in [\tilde{Q}_1, \tilde{Q}_3] \\ 0, & otherwise \end{cases} \quad (4)$$

The above indexing can be interpreted as a mapping of a matrix of continuum values, $\{h_{ij}\}_{i,j=1,\dots,N}$, into a matrix of discrete values $\{\omega_{ij}\}_{i,j=1,\dots,N}$.

The contribution of each pixel to surface roughness uniformity is computed by

$$p_{ij} = \frac{\omega_{ij}}{\sum_{i=1}^N \sum_{j=1}^N \omega_{ij}} \quad (5)$$

The topographic entropy is taken as the Shannon entropy,

$$H^{(2)} = -\sum_{i=1}^N \sum_{j=1}^N p_{ij} \log p_{ij} \quad (6)$$

where its normalized and centralized value is

$$H_{hei.matr}^{(2)} = \frac{H^{(2)} - H_{min}^{(2)}}{H_{max}^{(2)} - H_{min}^{(2)}} \quad (7)$$

since $H_{min}^{(2)} \leq H^{(2)} \leq H_{max}^{(2)}$. Now we need to compute $H_{max}^{(2)}$ and $H_{min}^{(2)}$. From the definition of η we have,

$$\sum_{i=1}^N \sum_{j=1}^N \omega_{ij} = N^2 - \eta \quad (8)$$

therefore

$$p_{ij} = \frac{\omega_{ij}}{N^2 - \eta} \quad (9)$$

The case $H_{max}^{(2)}$ corresponds to a uniform surface, $\eta_{min}=0$, hence $p_{ij} = 1/N^2, \forall(i, j)$, consequently

$$H_{max}^{(2)} = \log N^2 \quad (10)$$

The case $H_{min}^{(2)}$ corresponds to a surface with maximum η , that is $\eta_{max}=(1/2)N^2-2$ due to the region $[\tilde{Q}_1, \tilde{Q}_3]$ in boxplot has, at least, $(1/2)N^2+2$ pixels. As $N \gg 1$, we have $p_{ij}=1/(N^2/2)$ if $h_{ij} \in [\tilde{Q}_1, \tilde{Q}_3]$ or $p_{ij}=0$ otherwise. Therefore

$$H_{min}^{(2)} = \log(N^2/2) \quad (11)$$

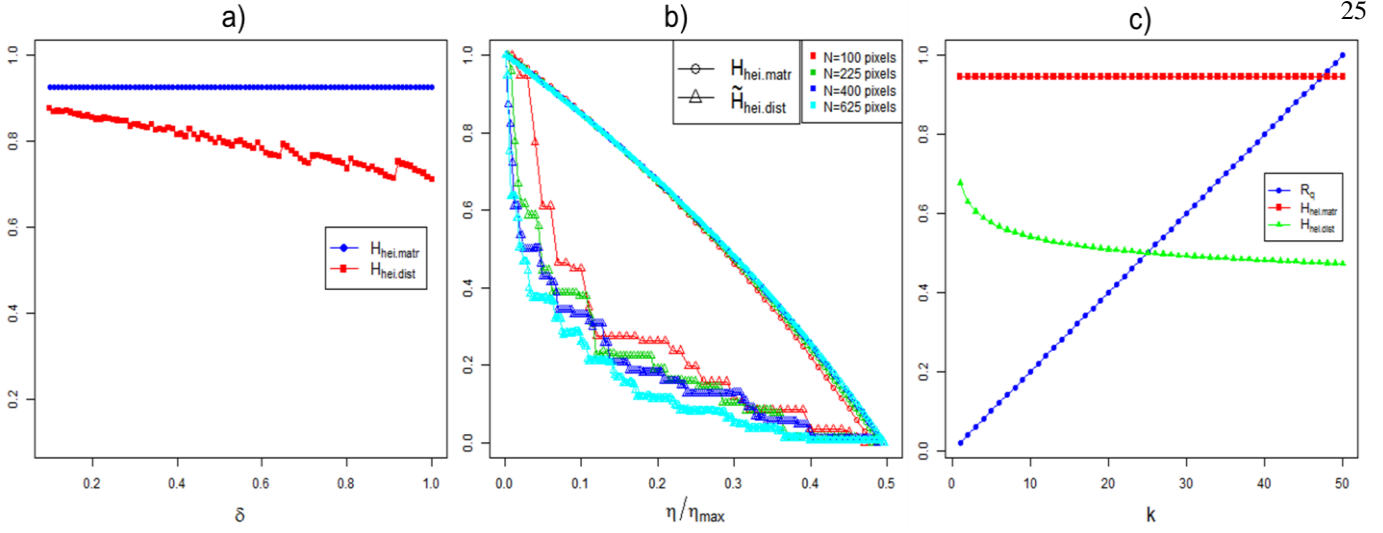


Figure 2: Results for the 3 simulations outlined in subsection 2.3.(a) The entropies from Eq. 3 and 7 as a function of size of bins δ . When δ increase $H_{hei.matr}$ remained steady, while $H_{hei.dist}$ decrease as an overall trend. (b) The dependence of $H_{hei.matr}$ and $H_{hei.dist}$ on the normalized nonuniformity η/η_{max} . Since $H_{hei.dist}$ does not depend directly on η we normalize and centralize $H_{hei.dist}$ for an effective comparison with $H_{hei.matr}$, i.e, we use $\tilde{H}_{hei.dist} = \frac{H_{hei.dist} - \min(H_{hei.dist})}{H_{hei.dist} - \max(H_{hei.dist})}$. Notice that $\tilde{H}_{hei.matr} = H_{hei.matr}$. Even though in different ways, both entropies decrease when η/η_{max} rises. (c) Effect of increasing h_{ij} by a multiplicative factor k on the measures R_q , $H_{hei.dist}$ and $H_{hei.matr}$. One can see that R_q and $H_{hei.dist}$ are negatively correlated, whereas $H_{hei.matr}$ and R_q are uncorrelated.

2.3 Numerical Simulation

Numerically, a random rough surface (RRS) can be generated by considering an initial mesh with $N \times N$ pixels which will receive heights driven by the following rules:

- i) $(x_i)_{i=1, \dots, N} \sim Unif(1, N)$
- ii) $(y_i)_{i=1, \dots, N} \sim Unif(1, N)$
- iii) $h(x_i, y_j)_{i, j=1, \dots, N} \sim Gau(\bar{h}, R_q)$

This means that there is no preferential direction on the plane x-y and surface heights are Gaussian distributed.

Once the RRS is generated, we compute both $H_{hei.dist}$ and $H_{hei.matr}$ for different δ , changing from δ_{min} to δ_{max} .

Afterwards, we evaluate the performance of $H_{hei.dist}$ and $H_{hei.matr}$ in detecting topographic uniformity through the ensuing steps:

- i) A RRS with $\eta_{min}=0$ is generated (uniform surface);
- ii) For each iteration, a generated $h'_{ij} \notin [\tilde{Q}_1, \tilde{Q}_3]$ replaces one $h_{ij} \in [\tilde{Q}_1, \tilde{Q}_3]$. In turn, it is computed $H_{hei.dist}$ and $H_{hei.matr}$;

iii) The step (ii) carries on until $\eta_{max}=(1/2)N^2-2$.

As the third numerical experiment we analyze the behavior of R_q , $H_{hei.dist}$ and $H_{hei.matr}$ when the height matrix increase by a multiplicative factor k , i.e. $h_{ij} \rightarrow kh_{ij}, \forall(i, j)$. The process $h_{ij} \rightarrow kh_{ij}$ will enables us to estimate the correlation between R_q , $H_{hei.dist}$ and $H_{hei.matr}$.

3 Results and discussion

In this section we present results and discussion on the numerical simulation described in Subsection 2.3. Furthermore, we consider two surface profiles to discuss in more details the relationship between entropy and surface roughness uniformity.

The common parameters throughout all simulations are: $\bar{h} = 0$, $R_q = 1$. In Fig. 2(a) the surface has 20×20 pixels and $0.1 \leq \delta \leq 1.0$, in Fig. 2(b) the surfaces have number of pixels from 10×10 to 25×25 and $\delta = 0.0001$, in Fig. 2(c) the surface has 20×20 pixels and $\delta = 0.0001$. All the codes were

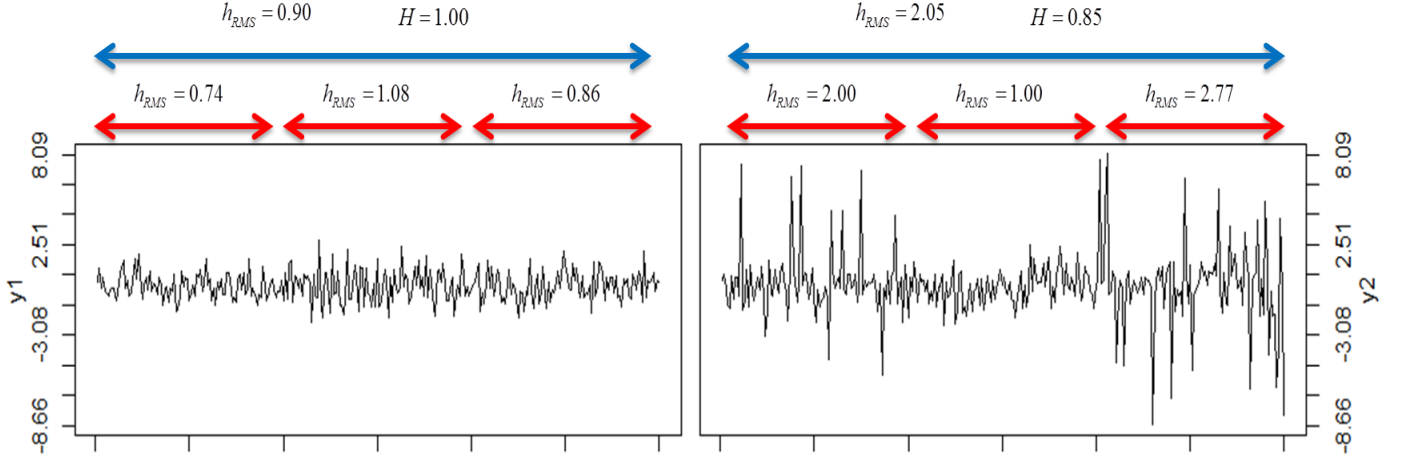


Figure 4: Two surface profile numerically generated. The blue line indicate that $H \in R_q$ were computed for the entire profile, while the red lines indicate the subregion considered for computing R_q . For these set of subregions the standart error, σ/\sqrt{n} , of R_q are $\varepsilon_{left}=0.10$ and $\varepsilon_{right}=0.51$.

implemented in programming language *R* [16].

Figure 2(a) shows how the measures $H_{hei.dist}$ and $H_{hei.matr}$ are affected when different choices of δ are taken. As expected, one can see that $H_{hei.matr}$ remained stable. On the other side, $H_{hei.dist}$ had some increases for certain δ , while this entropy declined as an overall trend.

Figure 2(b) shows how $\tilde{H}_{hei.dist}$ and $H_{hei.matr}$ change when the normalized quantity of nonuniformity on surface, η/η_{max} , rise. Both $\tilde{H}_{hei.dist}$ and $H_{hei.matr}$ decline when η/η_{max} increase, what is in accordance with our intuition for entropic measure: the smaller the uniformity, the smaller the entropy. However, such falls occur in distinct ways: $H_{hei.matr}$ drop monotonically, whereas $\tilde{H}_{hei.dist}$ decline sharply at the beginning, subsequently have some regions of constancy and slight decrease. Such differences between drops of $\tilde{H}_{hei.dist}$ and $H_{hei.matr}$ might be explained by the fact that one height matrix determines univocally one surface, whereas the same height distribution can be associated to distinct surfaces.

Figure 2(c) shows that $H_{hei.matr}$ stays constant when k increase, whereas $H_{hei.dist}$ decrease and R_q increase. The measures $H_{hei.dist}$ are R_q negatively correlated, $cor(R_q, H_{hei.dist}) = -0,867$, while R_q and $H_{hei.matr}$ are uncorrelated. Therefore $H_{hei.matr}$ can be taken as a complementary measure to R_q

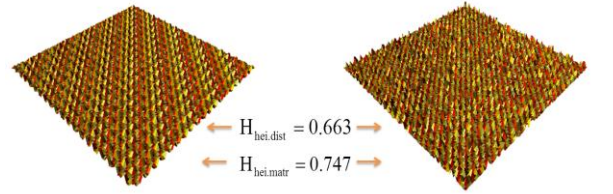


Figure 3: Both $H_{hei.matr}$ and $H_{hei.dist}$ do not take the height spatial distribution into account. In this case, two RRS were generated with the same height matrix and height distribution, but with different spatial configuration have the same $H_{hei.matr}$ and $H_{hei.dist}$.

It deserves to be noted that the entropy computed from Eq. 1 and 2 ignores the spatial correlation between the measurement points [9]. Such drawback is not solved by Eq. 5 and 6, as illustrated in Fig. 3.

As one can see in Fig 2 and Fig. 3 the values of $H_{hei.matr}$ and $H_{hei.dist}$ are not the same, in general. These differences can be explained by the fact that $H_{hei.dist}$ measures the uniformity regarding the uniform distribution $p(n_k)_{k=1,\dots,B} = 1/B$, while $H_{hei.matr}$ measures the uniformity regarding the bidimensional uniform distribution $p(x_i, y_j)_{i,j=1,\dots,N} = 1/N^2$.

Even though both $H_{hei.matr}$ and $H_{hei.dist}$ do not include spatial information about the pixels (i,j) , one can conclude from the findings in Fig. 2 that $H_{hei.matr}$ provides a more accurate way for ascertaining the topographic uniformity than $H_{hei.dist}$, since $H_{hei.matr}$ does not depend on an additional parameter, it has an univocal relationship with the uniformity degree and it is uncorrelated with R_q

Now, as pointed out since the Section 1, the entropic approach is related to the degree of surface roughness uniformity. Indeed, we can interpret the topographic entropy as a measure of how uniform is the set of heights distributed on the entire surface. As an example, let us consider two surface profile as illustrated in Fig. 4. For simplicity, we denote $H_{hei.matr}(profile\ k), k = 1, 2$ just by $H_k, k = 1, 2$. One can see that, in the left profile, the difference among the measured R_q in distinct subregion is not considerable ($\epsilon_{left}=0.10$) what lead a high entropy (in this case the maximum value). Nonetheless, the right profile has a substantial difference among the three subregions ($\epsilon_{right}=0.51$) what decrease the entropy.

4 Conclusion

We introduce the Shannon entropy as a measure of surface roughness uniformity. For numerically-generated randomly rough surface we compare the performance of estimation of the Shannon entropy from the height distribution, $H_{hei.dist}$ and from the height matrix, $H_{hei.matr}$, regarding three aspects: dependence on an additional parameter, sensibility to surface roughness uniformity and correlation with R_q . The results show that $H_{hei.matr}$ is better suited for quantifying surface roughness uniformity than $H_{hei.dist}$.

The measure $H_{hei.matr}$ can complement the information of R_q and consequently can contribute for characterization of rough surfaces.

It is important to stress that $H_{hei.matr}$ is not able to detect spatial configuration of pixels on surface. In this perspective, extending this methodology to a more general one would be interesting. Additionally, further research might investigate the direct interplay between topography uniformity and surface phenomena such as friction and adhesion.

References

[1]Yu, J. et al. Friction and adhesion of gecko-inspired PDMS flaps on rough surfaces Langmuir, 28, 2012.
 [2]Lorenz, B. et al. Adhesion: role of bulk viscoelasticity and surface roughness J. Phys.: Condens. Matter 25, 2013.
 [3]Assender, H. et al. How Surface Topography Relates to Materials' Properties, Science, 297, 2002.

[4]Persson, B.N.J et al. On the nature of surface roughness with application to contact mechanics, sealing, rubber friction and adhesion, J. Phys.: Condens. Matter, 17, 2005.
 [5]Blossey, R. Self-cleaning surfaces-virtual realities Nature Materials 297, 2, 2003.
 [6]Butt, H. J. et al. Force measurements with the atomic force microscope: Technique, interpretation and applications, Surface Science Reports, 59, 2005.
 [7]Bitler, A. et al. Fractal properties of macrophages membrane studied by AFM, Micron, 43, 2012.
 [8]Shannon, C. E. A Mathematical Theory of Communication, Bell Syst. Tech. J., 27, 1948.
 [9]Nosonovsky, M. Entropy in Tribology: in the Search for Applications, Entropy. 12, 2010.
 [10]Caticha A., Golan A. . An entropic framework for modeling economies, Physica A, 408, 2014.
 [11]Farina D., et al. The change in spatial distribution of upper trapezius muscle activity is correlated to contraction duration, Journal of Electromyography and Kinesiology, 18, 2008.
 [12]Kojadinovic I., J.-L. Marichal. Entropy of bi-capacities. European Journal of Operational Research, 178, 2007.
 [13]Ganeshana B. et al. Hepatic entropy and uniformity: additional parameters that can potentially increase the effectiveness of contrast enhancement during abdominal CT. Clinical Radiology, 62, 2007.
 [14]Zhou, Q. et al. A comparative study on clustering indices for distribution uniformity of nanoparticles in metal matrix nanocomposites, CIRP Journal of Manufacturing Science and Technology, 5, 2012.
 [15]Kam, K.M. et al. On assessing spatial uniformity of particle distributions in quality control of manufacturing processes, J Manuf. Syst., 32, 2012.
 [16]R Core Team R: A language and environment for statistical computing, Vienna, ISBN 3-900051-07-0, 2012.

**4 ESTUDO DA SUPERHIDROFOBICIDADE DE
FOLHAS DA ESPÉCIE VEGETAL *Thalia*
Geniculata (LINEU, 1753)**

(Artigo submetido à revista *Journal of Colloid and Interface Science*)